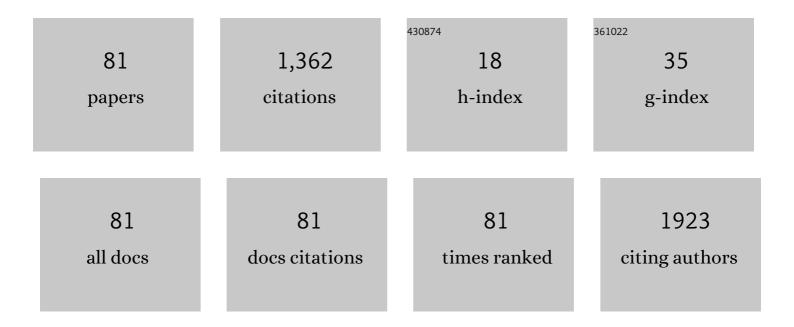
## Nazir P Kherani

List of Publications by Year in descending order

Source: https://exaly.com/author-pdf/10055758/publications.pdf Version: 2024-02-01



#	Article	IF	CITATIONS
1	Influence of metallo-dielectric optical properties on thermal resistance and solar heat gain coefficient of multi-pane glazing systems in hot and cold climates. Architectural Engineering and Design Management, 2022, 18, 894-910.	1.7	1
2	Ultraâ€Sensitive Cubicâ€ITO/Silicon Photodiode via Interface Engineering of Native SiO <i><sub>x</sub></i> and Latticeâ€Strainâ€Assisted Atomic Oxidation. Advanced Functional Materials, 2022, 32, .	14.9	6
3	Adiabatic mode transformation in width-graded nano-gratings enabling multiwavelength light localization. Scientific Reports, 2021, 11, 669.	3.3	4
4	Persistent CO2 photocatalysis for solar fuels in the dark. Nature Sustainability, 2021, 4, 466-473.	23.7	74
5	Asymmetric Metal-Dielectric Metacylinders and Their Potential Applications From Engineering Scattering Patterns to Spatial Optical Signal Processing. Physical Review Applied, 2021, 15, .	3.8	7
6	Multiâ€Functional Metasurface: Visibly and RF Transparent, NIR Control and Low Thermal Emissivity. Advanced Optical Materials, 2021, 9, 2100176.	7.3	11
7	Integrated Assembly and Photopreservation of Topographical Micropatterns. Small, 2021, 17, e2103702.	10.0	12
8	Integrated Assembly and Photopreservation of Topographical Micropatterns (Small 37/2021). Small, 2021, 17, 2170193.	10.0	2
9	Protein capture and SERS detection on multiwavelength rainbow-trapping width-graded nano-gratings. Nanotechnology, 2021, 32, 505207.	2.6	2
10	Rainbows at the End of Subwavelength Discontinuities: Plasmonic Light Trapping for Sensing Applications. Advanced Optical Materials, 2021, 9, 2100695.	7.3	12
11	Postâ€llumination Photoconductivity Enables Extension of Photoâ€Catalysis after Sunset. Advanced Energy Materials, 2021, 11, 2101566.	19.5	20
12	Plasmonic Titanium Nitride Facilitates Indium Oxide CO <sub>2</sub> Photocatalysis. Small, 2020, 16, e2005754.	10.0	32
13	Hydrogen Spillover to Oxygen Vacancy of TiO <sub>2–<i>x</i></sub> H <sub><i>y</i></sub> /Fe: Breaking the Scaling Relationship of Ammonia Synthesis. Journal of the American Chemical Society, 2020, 142, 17403-17412.	13.7	91
14	Tunable rainbow light trapping in ultrathin resonator arrays. Light: Science and Applications, 2020, 9, 194.	16.6	16
15	Black indium oxide a photothermal CO2 hydrogenation catalyst. Nature Communications, 2020, 11, 2432.	12.8	192
16	Solar-Driven Interfacial Water Evaporation Using Open-Porous PDMS Embedded with Carbon Nanoparticles. ACS Applied Energy Materials, 2020, 3, 3378-3386.	5.1	37
17	Optically and radio frequency (RF) transparent meta-glass. Nanophotonics, 2020, 9, 3889-3898.	6.0	8
18	High minority carrier lifetime in amorphous-crystalline silicon heterostructure using triode rf		0

PECVD. , 2020, , .

#	Article	IF	CITATIONS
19	Design, Fabrication and Optical Characterization of Photonic Crystal Patterned Ultra-Thin Silicon. , 2020, , .		1
20	Assembly of Topographical Micropatterns with Optoelectronic Tweezers. Advanced Optical Materials, 2019, 7, 1900669.	7.3	14
21	CO <sub>2</sub> Photoreduction: Heterostructure Engineering of a Reverse Water Gas Shift Photocatalyst (Adv. Sci. 22/2019). Advanced Science, 2019, 6, 1970134.	11.2	3
22	Multiwavelength Surfaceâ€Enhanced Raman Spectroscopy Using Rainbow Trapping in Widthâ€Graded Plasmonic Gratings. Advanced Optical Materials, 2018, 6, 1701136.	7.3	19
23	Enhanced photothermal reduction of gaseous CO <sub>2</sub> over silicon photonic crystal supported ruthenium at ambient temperature. Energy and Environmental Science, 2018, 11, 3443-3451.	30.8	83
24	Crystalline structure, electronic and lattice-dynamics properties of NbTe2. Scientific Reports, 2018, 8, 16984.	3.3	26
25	Ultrasmooth ultrathin Ag films by AIN seeding and Ar/N2 sputtering for transparent conductive and heating applications. APL Materials, 2018, 6, .	5.1	19
26	Patterned Optoelectronic Tweezers: A New Scheme for Selecting, Moving, and Storing Dielectric Particles and Cells. Small, 2018, 14, e1803342.	10.0	41
27	Solar Fuels: Tailoring Surface Frustrated Lewis Pairs of In <sub>2</sub> O <sub>3â°</sub> <i><sub>x</sub></i> (OH) <sub>y</sub> for Gasâ€Phase Heterogeneous Photocatalytic Reduction of CO <sub>2</sub> by Isomorphous Substitution of In <sup>3+</sup> with Bi <sup>3+</sup> (Adv. Sci. 6/2018). Advanced Science. 2018. 5. 1870034.	11.2	3
28	Kinetic analysis of nanoparticleâ€protein interactions using a plasmon waveguide resonance. Journal of Biophotonics, 2017, 10, 271-277.	2.3	3
29	Photothermal Catalysis: Photothermal Catalyst Engineering: Hydrogenation of Gaseous CO <sub>2</sub> with High Activity and Tailored Selectivity (Adv. Sci. 10/2017). Advanced Science, 2017, 4, .	11.2	2
30	Spectral plasmonic lensing of an array of metallic nanoslits. , 2017, , .		0
31	Carbon Dioxide Reduction: Visible and Near-Infrared Photothermal Catalyzed Hydrogenation of Gaseous CO2 over Nanostructured Pd@Nb2 O5 (Adv. Sci. 10/2016). Advanced Science, 2016, 3, .	11.2	1
32	Photoexcited Surface Frustrated Lewis Pairs for Heterogeneous Photocatalytic CO <sub>2</sub> Reduction. Journal of the American Chemical Society, 2016, 138, 1206-1214.	13.7	210
33	Low-temperature ozone-ambient grown native oxide passivation of crystalline silicon. , 2015, , .		0
34	Back amorphousâ€crystalline silicon heterojunction (BACH) photovoltaic device with facileâ€grown oxide ―PECVD SiN <sub>x</sub> passivation. Progress in Photovoltaics: Research and Applications, 2015, 23, 821-828.	8.1	6
35	Quantized structuring of transparent films with femtosecond laser interference. Light: Science and Applications, 2014, 3, e157-e157.	16.6	30
36	Reduction of Photoluminescence Quenching by Deuteration of Ytterbium-Doped Amorphous Carbon-Based Photonic Materials. Materials, 2014, 7, 5643-5663.	2.9	16

#	Article	IF	CITATIONS
37	Erbium-Doped Amorphous Carbon-Based Thin Films: A Photonic Material Prepared by Low-Temperature RF-PEMOCVD. Materials, 2014, 7, 1539-1554.	2.9	4
38	Design, fabrication and testing of a piezoelectric energy microgenerator. Microsystem Technologies, 2014, 20, 1035-1040.	2.0	24
39	Single mask fabrication process for movable MEMS devices. Microsystem Technologies, 2014, 20, 955-961.	2.0	1
40	Unimorph and bimorph piezoelectric energy harvester stimulated by β-emitting radioisotopes: a modeling study. Microsystem Technologies, 2014, 20, 933-944.	2.0	7
41	Light induced changes in the amorphous—crystalline silicon heterointerface. Journal of Applied Physics, 2013, 114, .	2.5	34
42	See-through amorphous silicon solar cells with selectively transparent and conducting photonic crystal back reflectors for building integrated photovoltaics. Applied Physics Letters, 2013, 103, 221109.	3.3	24
43	On controlling EBL parameters for nanoelectromechanical resonators fabricated on insulating/semiconducting structures. , 2013, , .		0
44	Novel method for fabricating high efficiency 10 μm thick c-Si solar cells. , 2013, , .		0
45	Stoichiometric amorphous hydrogenated silicon carbide thin film synthesis using DC-saddle plasma enhanced chemical vapour deposition. , 2013, , .		0
46	Facile nanometer thick native oxide based passivation of silicon for high efficiency photovoltaics. , 2013, , .		0
47	The augmented saddle field discharge characteristics and its applications for plasma enhanced chemical vapour deposition. Journal of Applied Physics, 2013, 113, .	2.5	18
48	High frequency SAW nanotransducer utilizing ultrananocrystalline diamond/ A1N bimorph architecture. , 2013, , .		0
49	Harnessing second-order optical nonlinearities at interfaces in multilayer silicon-oxy-nitride waveguides. Applied Physics Letters, 2013, 102, .	3.3	7
50	Optimal hydrogenated amorphous silicon/silicon nitride bilayer passivation of n-type crystalline silicon using response surface methodology. Applied Physics Letters, 2012, 101, 171602.	3.3	8
51	Ultrananocrystalline Diamond-Based High-Velocity SAW Device Fabricated by Electron Beam Lithography. IEEE Nanotechnology Magazine, 2012, 11, 979-984.	2.0	7
52	Absolute quantum yields in NaYF4:Er,Yb upconverters – synthesis temperature and power dependence. Journal of Materials Chemistry, 2012, 22, 24330.	6.7	31
53	Organic Light-Emitting Diodes: Silicon Nanocrystal OLEDs: Effect of Organic Capping Group on Performance (Small 23/2012). Small, 2012, 8, 3542-3542.	10.0	1
54	"Trapped Rainbow" effect within graded gratings for localization and detection of THz frequency components. , 2012, , .		0

#	Article	IF	CITATIONS
55	Nanocrystalline diamond/AlN structures for high efficient SAW nano-resonators. , 2012, , .		1
56	High-quality surface passivation of silicon using native oxide and silicon nitride layers. Applied Physics Letters, 2012, 101, .	3.3	35
57	15 GHz SAW nano-transducers using ultrananocrystalline diamond/AlN thin films. , 2012, , .		1
58	Modeling the performance of a micromachined piezoelectric energy harvester. Microsystem Technologies, 2012, 18, 1035-1043.	2.0	18
59	Gradient inverse opal photonic crystals via spatially controlled template replication of self-assembled opals. Nanoscale, 2011, 3, 4951.	5.6	19
60	Analysis and modeling of a bimorph AlN piezoelectric autonomous microgenerator stimulated by β-emitting radioisotopes. , 2011, , .		0
61	Self-irradiation enhanced tritium solubility in hydrogenated amorphous and crystalline silicon. Journal of Applied Physics, 2011, 109, .	2.5	1
62	Influence of the Electrode Spacing on the Plasma Characteristics and Hydrogenated Amorphous Silicon Film Properties Grown in the DC Saddle Field PECVD System. Materials Research Society Symposia Proceedings, 2011, 1321, 399.	0.1	0
63	Passivation study of the amorphous–crystalline silicon interface formed using DC saddleâ€field glow discharge. Physica Status Solidi (A) Applications and Materials Science, 2010, 207, 539-543.	1.8	15
64	Self-catalyzed Tritium Incorporation in Amorphous and Crystalline. Materials Research Society Symposia Proceedings, 2010, 1245, 1.	0.1	0
65	Power-scaling performance of a three-dimensional tritium betavoltaic diode. Applied Physics Letters, 2009, 95, .	3.3	33
66	Amorphous-crystalline silicon interface prepared using DC saddle-field pecvd. , 2009, , .		0
67	Back Amorphous-Crystalline Silicon Heterojunction (bach) photovoltaic device. , 2009, , .		12
68	Infrared Ellipsometry Investigation of Hydrogenated Amorphous Silicon. Materials Research Society Symposia Proceedings, 2009, 1153, 1.	0.1	1
69	Betavoltaics using scandium tritide and contact potential difference. Applied Physics Letters, 2008, 92,	3.3	20
70	Operational regimes of the saddle field plasma enhanced chemical vapor deposition system. Journal of Vacuum Science and Technology A: Vacuum, Surfaces and Films, 2008, 26, 462-471.	2.1	1
71	Tritiation of Semiconductor Materials for Micropower Application. Fusion Science and Technology, 2008, 54, 627-630.	1.1	1
72	Gamma-Free Smoke and Particle Detector Using Tritiated Foils. IEEE Sensors Journal, 2007, 7, 917-918.	4.7	15

#	Article	IF	CITATIONS
73	Photocarrier Radiometric Lifetime Measurements of Intrinsic Amorphous-Crystalline Silicon Heterostructure. Materials Research Society Symposia Proceedings, 2006, 910, 3.	0.1	1
74	Physical, electrical, and optical properties of SF-PECVD-grown hydrogenated microcrystalline silicon with growth surface electrical bias. Journal of Materials Science: Materials in Electronics, 2006, 17, 789-799.	2.2	3
75	Raman scattering characterization of SF-PECVD-grown hydrogenated microcrystalline silicon thin films using growth surface electrical bias. Journal of Materials Science: Materials in Electronics, 2006, 17, 801-813.	2.2	5
76	On-chip laser-locking of tritium in silica film using deep UV laser irradiation. , 2006, , .		0
77	Nuclear Batteries Using Tritium and Thin Film Hydrogenated Amorphous Silicon. Fusion Science and Technology, 2005, 48, 700-703.	1.1	6
78	Use of Tritium in the Study of Defects in Amorphous Silicon. Fusion Science and Technology, 2005, 48, 712-715.	1.1	1
79	Dependence of Microcrystalline Silicon Growth on Ion Flux at the Substrate Surface in a Saddle Field PECVD. Materials Research Society Symposia Proceedings, 2005, 862, 1961.	0.1	3
80	Harvesting Betavoltaic and Photovoltaic Energy with Three Dimensional Porous Silicon Diodes. Materials Research Society Symposia Proceedings, 2004, 836, L8.3.1.	0.1	0
81	Density of States in Tritiated Amorphous Silicon Measured Using CPM. Materials Research Society Symposia Proceedings, 2004, 836, L8.9.1.	0.1	0